"A Cochlear Nucleus Auditory prosthesis based on microstimulation"

Contract No. **No. NO1-DC-1-2105**
Progress Report #9

HUNTINGTON MEDICAL RESEARCH INSTITUTES
NEURAL ENGINEERING LABORATORY
734 Fairmount Avenue
Pasadena, California 91105

D.B. McCreery, Ph.D.
L.A. Bullara, B.S.
A.S. Lossinsky, Ph.D.

HOUSE EAR INSTITUTE
2100 WEST THIRD STREET
Los Angeles, California 90057

R.V. Shannon Ph.D
S. Otto M.S.
M. Waring, Ph.D

INTRODUCTION & ABSTRACT

The objective of this project is to develop central auditory prostheses based on an array of microelectrodes implanted into the ventral cochlear nucleus, in order to restore hearing to patients in whom the auditory nerve has been destroyed bilaterally. Our contract calls for the development of arrays of silicon substrate electrodes, which should allow placement of many more electrode sites into the human ventral cochlear nucleus than is possible with discrete iridium microelectrodes. We are developing an array for implantation into the human cochlear nucleus which has 16 electrode sites distributed on 4 silicon shanks extending from an epoxy superstructure that is 2.4 mm in diameter.

The probe shanks are either 2 or 3 mm in length. The 3 mm probes are intended to span the full tonotopic gradient of the human ventral cochlear nucleus, while the 2 mm shanks are appropriate for implantation into the feline ventral cochlear nucleus. To date, three of the 2 mm arrays have been implanted into the posteroventral cochlear nucleus 3 young adult female cats. One implant (CN144) continues to function after more than 130 days *in vivo*, although some the electrodes sites have become open circuited. We are working with the personnel at the Center for Neural Communications Technology to resolve this problem.

The performance of the array was followed by periodic measurement of the response growth functions (RGFs) evoked from each stimulating microelectrode sites and recorded in the inferior colliculus. In this cat, the slopes of the RGFs of some of the electrode sites still had not stabilized by 75 days after array implantation. However, the thresholds of the RGFs from several of the sites remained at or near 5 μA, when the stimulus pulse duration was 150 μs/phase, and near 10 μA with a pulse duration of 50 μs/phase. This is similar to what we have observed with discrete iridium microelectrodes implanted chronically in the feline PVCN.

When a single microelectrode sites was pulsed for 8 hours using a pulse train modulated by an artificial voice signal, the stimulated-induced depression of neuronal excitability (SIDNE) was minimal. However, when 2 adjacent microelectrode sites were pulsed, the SIDNE was quite severe, and was significantly greater than what we have observed when 4 discrete iridium microelectrodes, spaced 400 μm apart, are pulsed in the interleaved mode using similar parameters. Thus it appears that with these silicon probes, we must evaluate protocols that use a more restricted range of stimulus amplitudes.

The first human implantation of an array of discrete iridium penetrating microelectrodes occurred on July 24, 2003. The procedure revealed some problems with our strategy for targeting the ventral cochlear nucleus by using the Taenia choroidia as a landmark (the taenia is too wide in the rostral-caudal dimension) and with the routing of the cable from the penetrating array. Thus only one of the penetrating microelectrodes produced an auditory percept, and we did not achieve a true multi-channels device. However, the threshold of the auditory percept was low (< 1 nC), as predicted from the animal studies, and the dynamic range was quite large. The patient has suffered no ill effects attributable to the penetrating array and is benefitting from the device, which include both the penetrating and a surface electrode array. We have revised our procedure for targeting the human ventral cochlear nucleus and we have modified the inserter tool so that the cable from the penetrating array can be over the surface of the brainstem.

I: Development of an array of silicon substrate electrodes

I.1 Background & Methods

The objective of this project is to develop central auditory prostheses based on an array of microelectrodes implanted into the ventral cochlear nucleus, in order to restore hearing to patients in whom the auditory nerve has been destroyed bilaterally. Our contract calls for the development of arrays of silicon substrate electrodes, which should allow placement of many more electrode sites into the human cochlear nucleus than is possible with discrete iridium microelectrodes. We are developing an array for implantation into the human cochlear nucleus that has 16 electrode sites distributed on 4 silicon shanks extending from an epoxy superstructure that is 2.4 mm in diameter. This is the same footprint as our first- generation human arrays employing discrete iridium microelectrodes and is designed to be implanted using the same inserter tool. The silicon probes are fabricated at the University of Michigan under the direction of Design Engineer Jamille Hetke, and are provided through the Center For Neural Communications Technology (U of M). The 2 mm shanks are appropriate for implantation into the feline ventral cochlear nucleus. Figure I-1 shows a probe with 2 of the 2 mm shanks, each with four 2,000 μm^2 iridium electrode sites distributed between 0.8 and 1.7 mm below the horizontal spine. A stainless-steel pin is affixed to the rear of the probe, and embedded in a backing of EpoTek 301 epoxy. The pin is used in the handling of the probes and to align the probe shanks when the probe is incorporated into an array. After the pin and the EpoTek backing have been applied to the rear of the horizontal spine, the electrical lead wires are bonded to the pads on the probe spine, and the junctions are insulated with Nusil 4211 silicon elastomer, as shown in Figure I-1 Figure I-2 shows an array with 2 of the probes (4 shanks and 16 sites) extending from an epoxy (EpoTek 301) superstructure which floats on the dorsal surface of the cochlear nucleus. The array's cable is angled vertically, to accommodate the transcerebellar approach to the feline cochlear nucleus.

The surgical implantation of the arrays into the feline postero ventral cochlear nucleus (PVCN) was described in QPR#7. Using general anesthesia and aseptic technique, a small craniectomy is made over the left lateral cerebellum just posterior to the tentorium. The rostro-lateral portion of the cerebellum is aspirated using small pipettes, to expose the dorsal surface of the cochlear nucleus. The upper surface of the array's epoxy superstructure is positioned on the end of a vacuum wand mounted on a stereotaxic electrode carrier and advanced into the dorsolateral surface of the cochlear nucleus. The recording electrode is inserted by stereotaxis into the extreme rostral end of the right inferior colliculus, in order to broadly sample inputs from the cochlear nucleus. The recording reference electrode is implanted dorsal to the right inferior colliculus.

Cat CN144 was followed for 114 days after implanting the electrode array and remains alive at the time this report was written. At intervals after implantation, the cat

was anesthetized lightly with Propofol and the responses evoked from each of the microelectrodes in the left PVCN were recorded via the electrode in the rostral pole of the right inferior colliculus. The stimulus was cathodic-first, charge-balanced pulse pairs, each phase 150 μs in duration. 1024 successive responses were averaged to obtain each averaged evoked response (AER, Figure I-3). Because of its short (~ 1 ms) latency after the stimulus, the 1st component of the AER shown in Figure 3 is assumed to represent neuronal activity evoked directly in the neurons projecting from the PVCN to the inferior colliculus, while the second component may represent neuronal activity that is evoked transsynaptically. The response growth functions (RGFs), which represent the recruitment of the neural elements surrounding the microelectrode, were generated for each stimulating electrode site in the PVCN, by plotting the amplitude of the first component of each of the AERs evoked from the site, against the amplitude of the "probe" stimulus that evoked the AER.

We compared the change in the electrical excitability of the neurons in the PVCN when only one electrode site, and also when two adjacent electrode sites are pulsed for 8 hours. For the prolonged stimulation regimen, we have simulated an acoustic environment based on a computer-generated artificial voice that was specified and provided by the International Telegraphic & Telephony Consultive Convention, for the purpose of testing telecommunication equipment (CCITT, 1988). The CCITT artificial voice reproduces many of the characteristics of real speech, including the long-term average spectrum, the short-term spectrum, the instantaneous amplitude distribution, the voiced and unvoiced structure of speech, and the syllabic envelope. The artificial voice signal was passed through a full wave rectifier and then underwent logarithmic amplitude compression, before being sent through an appropriate anti-aliasing filter. The range of pulse amplitudes was adjusted so that acoustic silence is represented by a pulse amplitude that is close to the threshold of the response recorded in the central nucleus of the inferior colliculus while stimulating in the PVCN. The artificial voice signal was presented for 15 seconds, followed by 15 seconds in which the stimulus amplitude was held near the threshold of the evoked response. This 50% duty cycle is intended to simulate a moderately noisy acoustic environment. The amplitude of the signal from the filter then sets the amplitude of the charge-balanced stimulus pulses, which were delivered to each electrode at 250 Hz per electrode. In the session in which 2 electrode sites were pulsed, each site received the same stimulus, but with the stimulus pulses interleaved. We have used this artificial voice signal in our previous studies of prolong intranuclear microstimulation (McCreery et al, 1997, 2000). We used a pulse duration of 50 μs/phase, and the artificial voice signal ranged between 10 and 48 μA. This regimen will induce measurable depression of neuronal excitability when applied through 4 discrete iridium microelectrodes spaced 400 μm apart in the PVCN.

The stimulation and data acquisition were conducted using a two-way radiotelemetry stimulation and data acquisition system, and the cats are able to move about freely in a large Lucite cage. This telemetry system and its companion software allow continuous monitoring of the voltage waveform across the stimulating microelectrodes, and of the compound evoked potential induced in the inferior

colliculus by the stimulating microelectrodes.

RESULTS

Figure I-4 shows the location of several of the electrode sites on the array implanted into cat CN144. The response growth functions (RGFs) were measured over a range of current amplitudes between 0 and 35 μA. The thresholds of the RGFs from electrodes sites 5 and 9 on the rostro-lateral shank were the lowest. The connection to site 1 on the rostral -lateral shank was electrically open, but the connections to the shallowest sites on the other 3 shanks were intact, and the RGF from site 3 on the caudal-medial shank were recorded. Figure I-5A and I-5B show the RGFs recorded at 75 and 105 days after array implantation. In cat CN144, the RGFs had not stabilized fully even by 75 days after implantation of the array. Between 75 and 105 days, the RGF from electrode site 5 was virtually unchanged, while the slope of the response from site 9 had decreased significantly and that of the response from site 3 increased. However, the thresholds of the three curves remained at approximately 5 μA.

At 114 days after implantation of the array, the two adjacent electrode sites on the rostro-lateral shank (sites 5 and 9) were pulsed for 8 hours, in the interleaved mode, at 250 Hz per electrode, using the artificial voice signal described above. For this experiment, we used a pulse duration of 50 μs/phase. With the shorter pulsed duration, the responses are shifted to slightly higher currents, and this is more compatible with the amplitude quantitation of the Nucleus 24 stimulator/receiver, which will be used for any future the human trials. Figure I-6A shows the RGFs evoked from the two sites, recorded before and after the 8 hours of stimulation. There was marked depression of neuronal excitability (SIDNE), around both electrode sites. By 13 days after the stimulation (127 days after array implantation), the electrical excitability of the sites had recovered, and the 8-hour stimulation was repeated, but now only electrode site 9 was pulsed, at 250 Hz (Figure 6B). The SIDNE was much less marked than when both sites were pulsed (Figure I-6A), and by 24 hours after the end of stimulation, the RGF had nearly recovered.

DISCUSSION

The amount of SIDNE depicted in Figure I-5A is significantly greater than what we have observed when 4 discrete iridium microelectrodes, spaced 400 μm apart, are pulsed in the interleaved mode using similar parameters (McCreery et al, 2000). This difference might be attributed to the slightly closer spacing of the electrodes sites on the silicon probe (300 μm) and to the fact that the current field might be “focused” slightly by the non-conductive silicon shank. Both factor would result in greater overlap of the stimulus fields. In the cerebral cortex, we have observed a “mass-action” component to SIDNE, when many closely spaced microelectrodes are pulsed either simultaneously or in the interleaved mode (McCreery et al, 2001). In the feline cochlear nucleus, SIDNE is much more severe when a single microelectrode is pulsed at 500 Hz, vs 250 Hz. When there is significant overlap of the effective current fields from 2 electrodes that are pulsed sequentially at 250 Hz, the effective stimulus frequency is 500 Hz. Since the functionality of an auditory prosthesis may be compromised significantly by reducing the pulsing rate below 250 Hz/electrode, it appears that with these silicon probes, we must evaluate protocols that use a more restricted range of

stimulus amplitudes.

In the present array, several of the microelectrode sites became open circuited during the time *in vivo*. We also have experienced some problems with delamination of gold clad from the bonding pad on the probes spines. We are modifying our procedure for attaching the platinum-iridium lead wires to the bonding sites, and we are working with the personnel at the University of Michigan to resolve the delamination problem

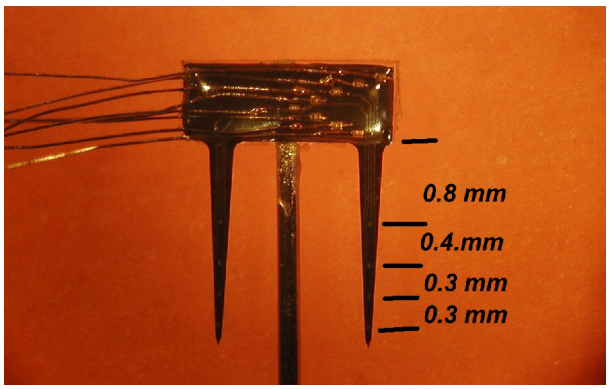

Figure I-1

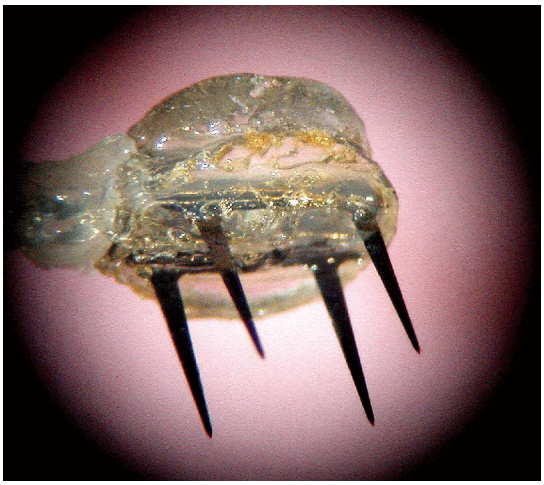

Figure I-2

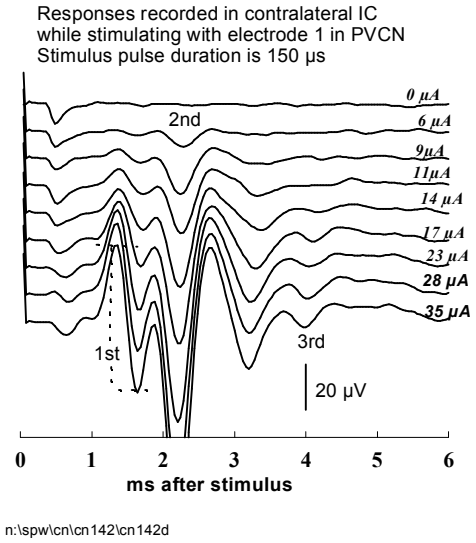

Figure I-3

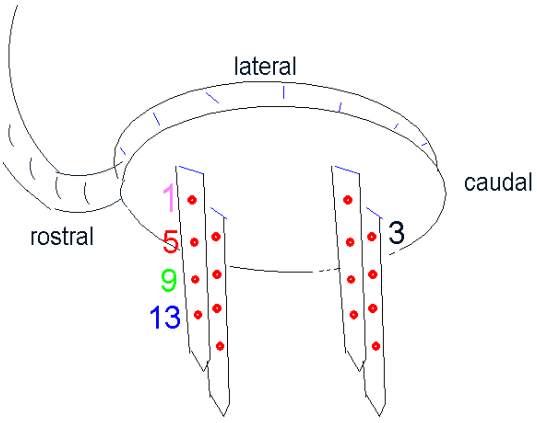

Figure I-4

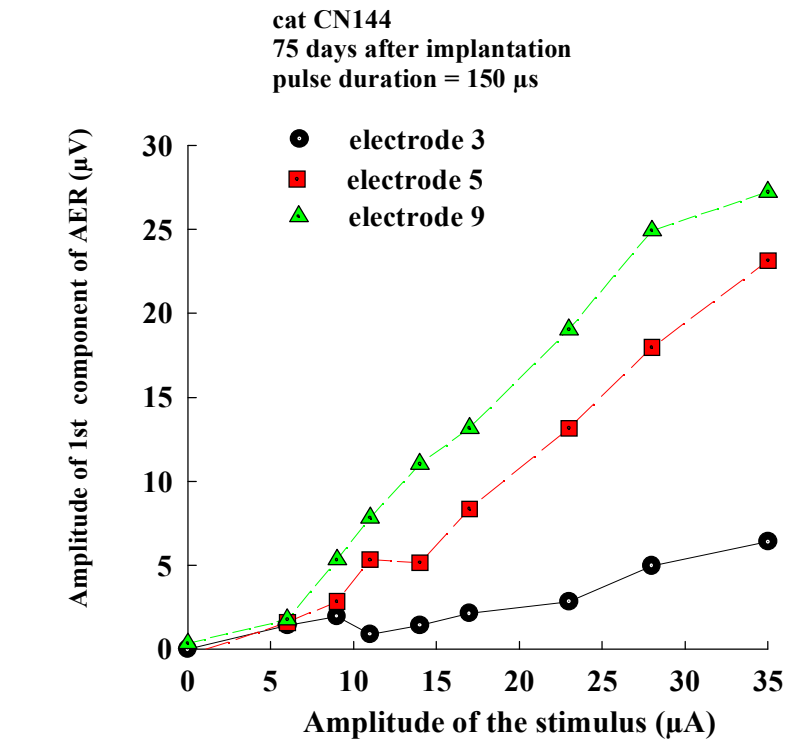

n:\spw\cn\cn144\cn144a1.spw

Figure I-5A

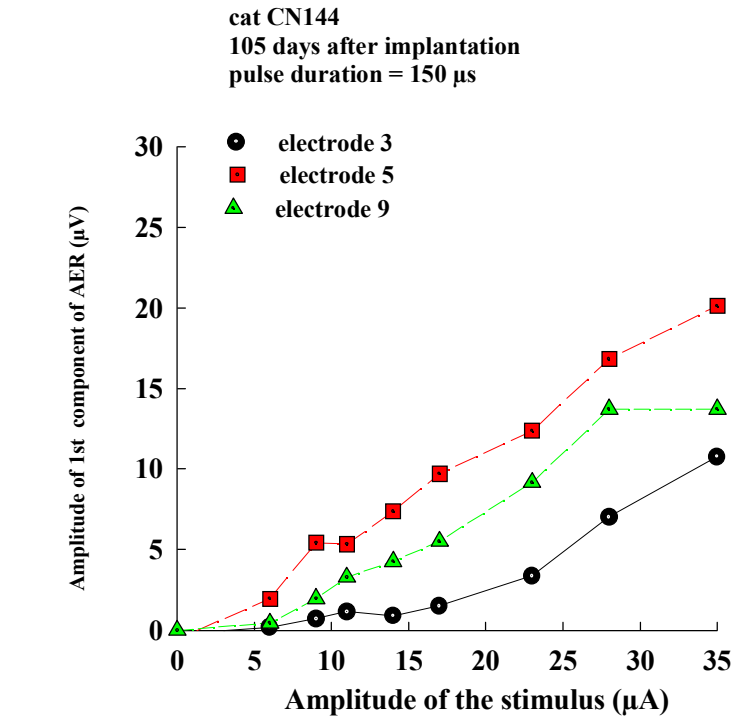

n:\spw\cn\cn144\cn144c1.spw

Figure I-5B

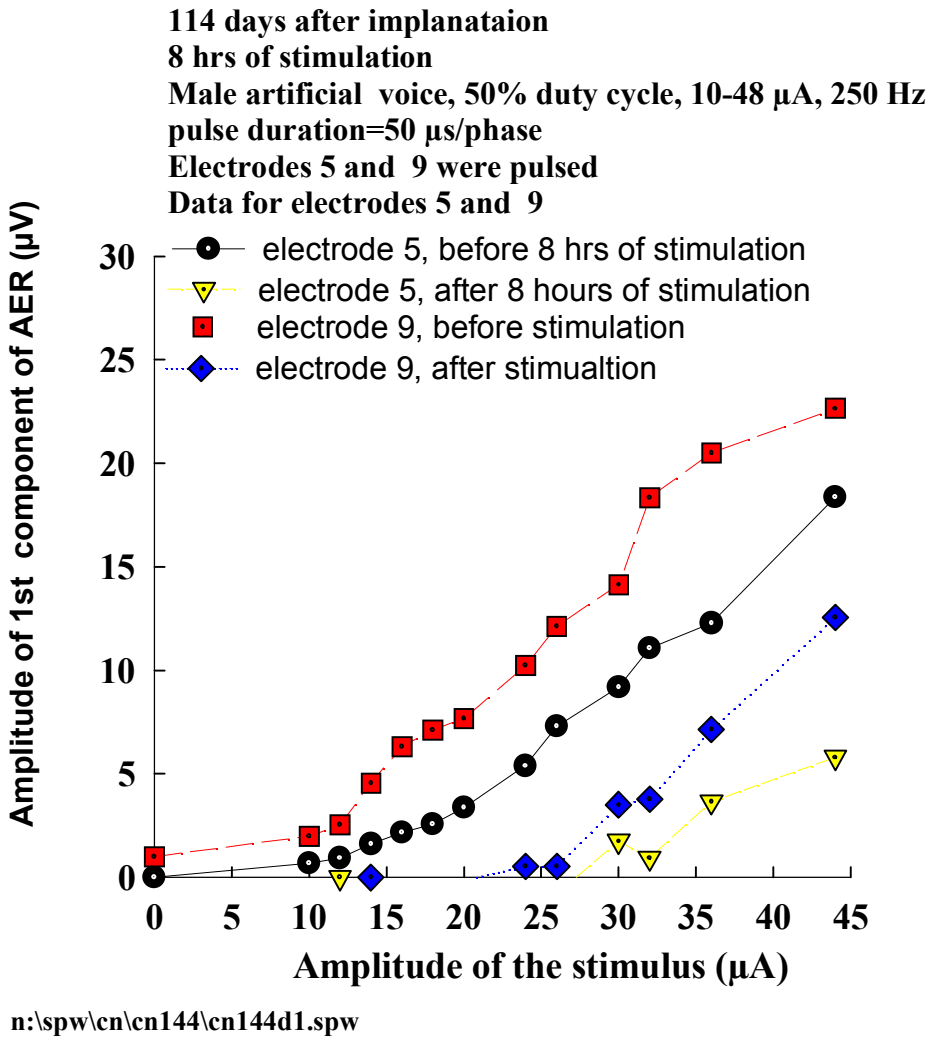
114 days after implanataion
8 hrs of stimulation
Male artificial voice, 50% duty cycle, 10-48 µA, 250 Hz
pulse duration=50 µs/phase
Electrodes 5 and 9 were pulsed
Data for electrodes 5 and 9
electrode 5, before 8 hrs of stimulation
electrode 5, after 8 hours of stimulation
electrode 9, before stimulation
electrode 9, after stimualtion
Amplitude of 1st component of AER (µV)
Amplitude of the stimulus (µA)
0
5
10
15
20
25
30
35
40
45
n:\spw\cn\cn144\cn144d1.spw

Figure I-6A

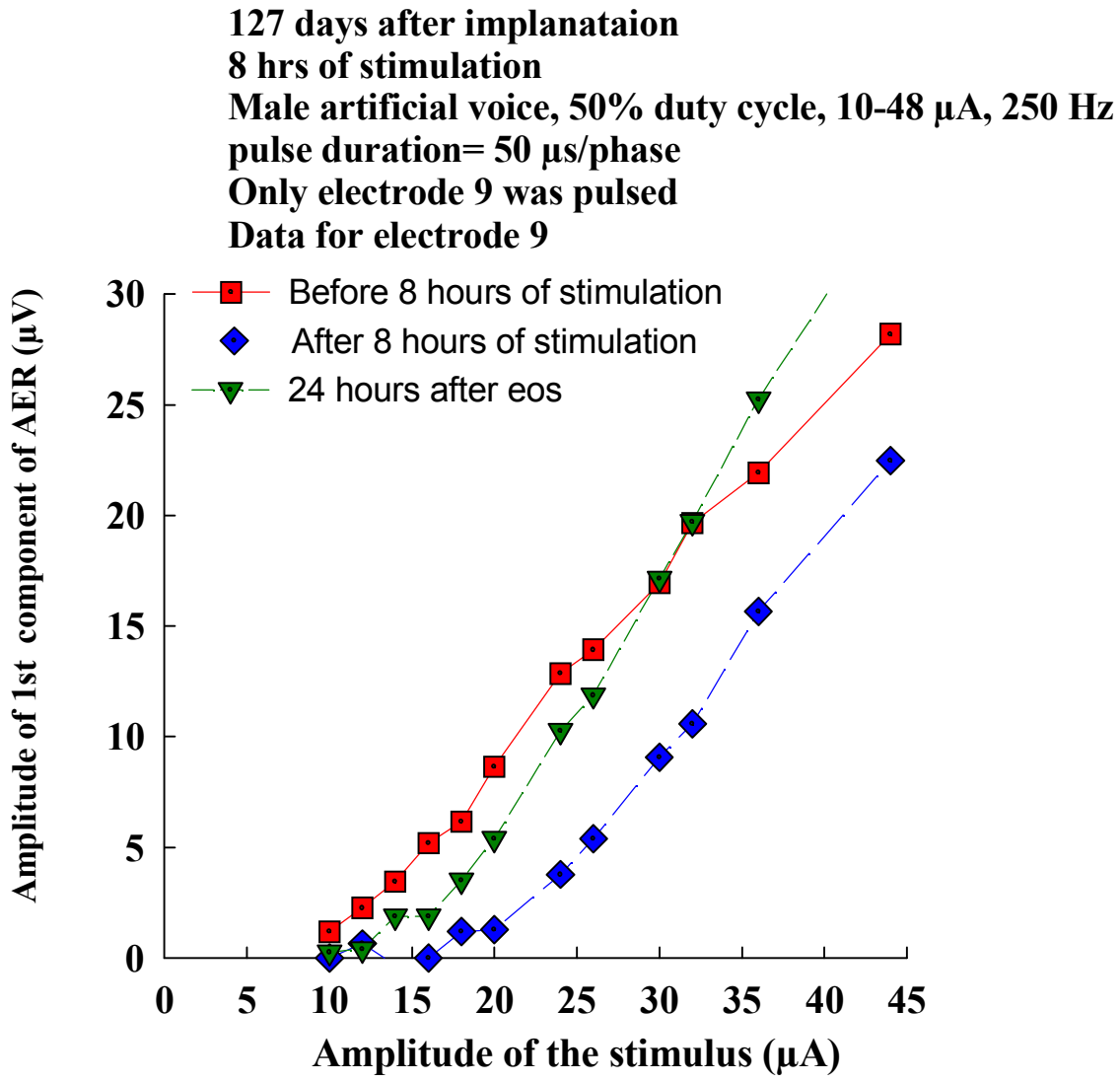

n:\spw\cn\cn144\cn144k1.spw

Figure I-6B

II: Human Implantation of a microelectrode array

PABI Patient Selection

Patients selected for participation in the penetrating auditory brainstem implant(PABI) project are all patients at the House Ear Clinic with Type II neurofibromatosis (NF2) who present for removal of bilateral vestibular schwannomas (VS). There are no audiological criteria because any remaining hearing will be lost following tumor removal. Patients are implanted following protocols approved by the St. Vincent Medical Center and Huntington Memorial Hospital (Pasadena, CA) Institutional Review Boards. Candidates are counseled extensively prior to surgery regarding the limitations, risks, and benefits of the PABI. They view a 50-minute video presentation featuring three recipients of the surface ABI. They also have ample opportunity to review and discuss the PABI informed consent form, which contains several illustrations of the device and explains its function. Individuals are considered candidates if their expectations are reasonable, and they indicate ability and willingness to comply completely with the extensive follow-up protocol.

The first PABI recipient (PABI#1) is a 19 year old female from Utah. She has a very quiet personality, and usually does not initiate conversation. Her parents report that she has a very mild articulation anomaly from childhood, which we noted didn't significantly affect our ability to understand her speech.

PABI#1's parents are very supportive of her and highly enthusiastic about her participation in the PABI clinical trials. They have kept in touch with us via regular e-mails and report the patient is using her ABI continuously with benefit. They reported recently that she enjoyed using her ABI at a band, orchestra, and choral concert. She reported that although she could detect the musical sounds, she was not able to distinguish music from singing or speaking. This is typical of early ABI use. She also used her PABI at a movie which she was able to follow reasonably well. She continues to work at a deaf pre-school where she worked prior to implantation and her fellow teachers have noted that they are seeing improvements in her auditory performance with her PABI.

Surgical procedure

The implant includes the Nucleus 24 stimulator/receiver and the arrays of surface and penetrating electrodes (Figure II-1,2). Surgical access for the PABI is via a translabyrinthine approach, the same as is used for the surface electrode ABI. This surgical approach is commonly used for access to the cerebello-pontine angle for removal of vestibular schwanomas and it provides good visibility of the anatomical structures relevant to ABI and PABI placement (Brackmann et al, 1993). Following tumor removal the receiver-stimulator is seated in a recess drilled in the mastoid. The lateral recess (LR) of the IV ventricle is localized and the surface ABI electrode array is inserted. The device is stimulated and evoked responses are recorded from electrodes on the scalp. If auditory evoked potentials are not observed the electrode is repositioned in the

LR and Polyester felt is positioned behind the electrode array to hold it in contact with the wall of the LR. Once a satisfactory placement has been achieved for the surface electrode array, the penetrating PABI array is loaded into the insertion tool. The neurosurgeon positions the tip of the insertion tool adjacent to the mouth of the LR near the taenia choroidia and injects the penetrating array. The leads for both penetrating and surface electrode arrays are then packed into the surgical opening and the surgical opening is closed in layers. This procedure was completed without incident. No significant bleeding was observed around the penetrating array and no change was observed in any monitoring equipment or in any vital signs. Once placed, the penetrating array appeared to be stable in location, at while it remained visible during the procedure.

Threshold and Dynamic Range

Thresholds and the upper limit of comfortable loudness were measured using a standard audiological method. The patient was instructed to listen for a soft pulsing sound or to report if they felt any non-auditory sensation. Following the first report of an audible sound the level was reduced to the level at which the patient could accurately report the number of stimulation bursts. If a non-auditory sensation was encountered, stimulation was discontinued on that electrode and the patient was asked to describe the quality, location, and magnitude of the non-auditory sensation. Maximum comfortable loudness level was measured by slowly increasing the stimulation level and asking the patient to report the loudness level on a numerical scale of 0-10. Patients were instructed to report any non-auditory sensations. If no non-auditory sensations were encountered the stimulation level was increased until the patient reported the loudness level to be loud, but not uncomfortably loud. This stimulation level was recorded as the maximum comfortable loudness level (MCL). Thresholds were measured with 300 us/ph biphasic pulses for the surface electrodes and with 25 us/phase biphasic pulses for the penetrating microelectrodes.

Figure II-3 presents thresholds and MCL in nano-Coulombs for all electrodes for which auditory sensations could be obtained. Electrodes 3, 6, 9, 12, 15, 18 and 21 were along one side of the surface array, electrodes 2, 5, 8, 11, 14, 17 and 20 were along the other edge of the surface array, and electrodes 1, 4, 7, 10, 13, 16, 19 and 22 were located on the penetrating array. Open circles in Figure 3 present thresholds and MCLs from one edge of the surface array, open triangles present data from the other edge of the array, and filled triangles present data from the penetrating electrodes. For each electrode the two points connected by a line indicate the threshold and MCL for that electrode.

Auditory percepts were obtained from only one of the 8 penetrating electrodes and from 11 of the 14 surface electrodes. The penetrating electrode that did produce the auditory percepts was at the edge of the array, suggesting that the array was inserted at the extreme edge of the cochlear nucleus. Non-auditory side effects from the surface and penetrating electrodes were generally perceived as tingling sensations on the ipsilateral side of the body, primarily in

the ipsilateral hand, which we interpret as antidromic activation of the inferior cerebellar peduncle, a structure in close proximity to the cochlear nucleus in humans. Note that the threshold charge for the penetrating electrode was less than 1 nC, a level that indicates that the electrode was in close proximity to auditory neurons. Threshold levels from the penetrating electrode were considerably lower than threshold levels observed on the surface electrodes. A wide dynamic range (more than 10 dB) was observed on the penetrating electrode and on one of the surface electrode. All other electrodes exhibited the small dynamic range typical of surface-electrode ABI stimulation (Shannon, 1989).

An interesting pattern of thresholds was observed for the surface electrode array: the lowest threshold level occurred in the middle of the array and threshold levels increased progressively towards the medial and lateral ends of the array. A simple inverse-square law model was applied to the data as shown by the line in Figure 3. This model assumed that all stimulation was occurring at a location close to the middle electrode. As the distance from electrode 12 increased the model assumed that the level of the stimulation must be increased by an amount that was proportional to the square of the distance. This model assumes a simple inverse square law for threshold current as a function of distance from the stimulating electrode. Thus to achieve a threshold current at a particular distance from electrode 12, the current must be proportional to the square of the distance from electrode 12. The line in figure 3 assumed a current spreading constant of 0.7. This simple model provides an excellent fit to the data, suggesting that all threshold currents along that side of the surface array were actually producing activation at one location – near electrode 12. Thresholds on the opposite side of the surface array (open triangles) showed a similar pattern, but many of the electrode on that side of the array also produced non-auditory side effects.

Intensity Discrimination

Intensity discrimination measures the smallest change in electrical current that produces a perceptually discriminable change in loudness. Previous ABI results have shown that electrical stimulation allows approximately 10-20 discriminable steps in loudness across the dynamic range (compared to more than 200 for acoustic hearing). Some ABI patients appear to have as few as 4 discriminable steps in intensity between threshold and MCL. It was anticipated that penetrating microstimulation would produce a larger dynamic range and more discriminable steps withing that range, due to the more orderly recruitment of neurons around the electrode when compared to a surface electrode.

Intensity discrimination was measured in a 2-alternative, forced-choice (2AFC) adaptive method. The patient was presented with two stimulation bursts, each 200 ms in duration. Each stimulus was indicated by a flashing icon on the screen as it occurred. The patient was instructed to indicate which of the two sounds was louder by clicking on the appropriate icon with a mouse. The difference in stimulation was increased following each incorrect response and decreased following three correct responses in a row. This sequence will

converge on the stimulus level at which the listener would achieve 79% correct. Each data point represents the average of 8 reversals after discarding the first 4 reversals.

Figure II-4 presents intensity difference limens (DL in dB) as a function of the level of the standard stimulus above threshold (dB SL). Open symbols present data from previous ABI patients (Shannon and Otto, 1990) and filled symbols present intensity DLs from PABI #1. Intensity DLs were measured for the penetrating electrode (P16) and for a surface electrode that was roughly similar in pitch to the penetrating electrode (S21). Note that the DLs for the penetrating electrodes were larger than typical DLs for previous surface electrode ABIs and larger than the DLs from the surface electrode in this same patient. However, the surface electrodes had smaller dynamic ranges than the penetrating electrode, so that the number of discriminable steps in intensity may not be different.

Gap Detection

One measure of temporal resolution is the ability to detect a brief gap in an ongoing sound. Normal-hearing listeners can typically detect a gap of a few ms at most loudness levels, and require a gap of 10-20 ms for detection with very soft sounds. Cochlear implant patients can detect a gap of 20-40 ms in soft sounds and a gap of 2-3 ms in medium -to- loud sounds. Average data from 38 cochlear implant listeners is presented in Figure II-5, as a hatched area. Data from 8 ABI patients with surface electrode arrays is shown in the top panel of Figure 5 for comparison (Shannon and Otto, 1990). In general, ABI patients showed a similar pattern of gap detection to cochlear implant users. All of the data presented in Figure II-5 was collected with a 2AFC adaptive technique to estimate the 70.9% correct level.

Gap Detection results from PABI#1 are shown in the lower panel of Figure II-5. Results are shown for two surface electrodes (S3 and S21) and for two repetitions of the task for the penetrating electrode (P16). In general PABI#1's gap detection thresholds were a bit longer than typical ABI listeners at all loudness levels. It is not clear if this reflects a poor ability to detect gaps in this patient, or if it simply represents a lack of experience with the listening task. All other data in Figure II-5 was collected from patients with considerable experience with their implant device and from subjects who were relatively experienced in the gap detection psychophysical task. However PABI#1 had only used the PABI speech processor for one day at the time of testing and had no prior experience with psychophysical tasks. Gap detection measures will be repeated for PABI#1 at the next follow-up testing session to determine if the gap detections thresholds decrease after a period of experience with the device or with more experience in a psychophysical task.

Modulation Transfer Functions

Another measure of temporal resolution in hearing is the temporal modulation transfer function (TMTF). This technique measures the threshold for the detection of modulation as a function of the modulation frequency. In

listeners with normal hearing (NH), modulation detection is best at low modulation frequencies and becomes poorer as the modulation frequency increases above 60 Hz. The dashed line in Figure II-6 shows TMTFs from persons iwth normal hearing (Bacon and Viemeister, 1985). Cochlear implant listeners have similar TMTFs, although they might be a bit better at detecting modulation at 100 Hz than are persons with normal hearing. The top panel of Figure II-6 shows TMTFs from previous ABI listeners with a surface electrode array (Shannon and Otto, 1990). On average, ABI patients' TMTFs were similar to those of listeners with normal hearing. All TMTF results were measured with a 2AFC tracking procedure in which the depth of modulation was adaptively changed to converge on the modulation depth that would produce 70.9% correct detection.

TMTFs from PABI#1 are shown in the lower panel of Figure II-6. TMTFs were measured for a 250 pps carrier for the penetrating electrode (P16) and for both a 250 pps and 1000 pps carrier for a pitch-matched surface electrode (S21). Overall, PABI#1 required larger modulation depths for detection than persons with normal hearing, or persons with cochlear implants, or previous ABI patients. There was no clear difference between modulation detection with the surface or penetrating electrodes. Again, it is not clear if this poor performance is patient specific, or simply reflects a lack of experience with electrical stimulation and/or psychophysical tasks. These measures will be repeated on subsequent test sessions to assess the effects of experience.

Forward Masking

Another measure of temporal processing is forward masking, which measures the recovery of adaptation following a masker. A masker is presented at a medium-loud level for 200 ms and then turned off. The threshold of a brief (20 ms) signal is measured as a function of the time delay of the signal following masker offset. Signal threshold was measured with a 2AFC adaptive procedure to estimate the level of 70.9% correct detection.

The upper panel of Figure II-7 presents forward masking results from 20 cochlear implant listeners and from 7 previous ABI users with surface electrodes (Shannon and Otto, 1990). Normalized signal level is plotted vs the logarithm of time delay between masker offset and signal onset. Amplitudes were normalized due to the large differences across subjects and electrodes in threshold and dynamic range. The normalization was based on threshold and MCL for a 20 ms signal. On these coordinates forward masking recovers approximately linearly for both cochlear implant and ABI listeners, recovering to quiet threshold level (showing no residual adaptation) by 300-500 ms. If NH forward masking functions are normalized in a similar fashion (but in dB) they also recover linearly with about the same recovery time constant.

Forward masking data from PABI#1 is presented in the lower panel of Figure II-7 for the penetrating electrode and three surface electrodes. These curves appear to be higher than the average from cochlear implant users, but the curves from PABI#1 have not been properly normalized. Data from cochlear implant users were normalized relative to the threshold and dynamic range of a

20 ms signal. Thresholds were only obtained from PABI#1 for 200 ms signals, which are typically lower than thresholds for a 20 ms signal due to temporal integration. Thus, the plotted data in Figure 7 shows normalized threshold levels that are higher than the comparison data from cochlear implants. Once thresholds are obtained for 20 ms signals, we expect the forward masking recovery curves to be shifted down. Observe that the PABI forward masking functions show approximately linear recovery with approximately the same time constant as the cochlear implant users. After proper normalization it is expected that the PABI functions will be similar to those from persons with normal hearing, cochlear implants and previous ABI users. There is also no difference in the recovery functions for surface electrodes (S3, S12, S21) and the penetrating electrode (P16). While no firm conclusions can be drawn prior to proper normalization, we do not anticipate that forward masking in PABI#1 is any different than other listeners with the surface ABI, and that there will be no difference between penetrating and surface electrodes.

Speech Recognition Results

Following the initial assessment of non-auditory side effects and the measurement of threshold and MCL on each electrode, PABI#1 was fit with several speech processor strategies. Four speech processors were fitted and performance measured on speech recognition tasks. In all processors the electrodes used were loudness-balanced and ordered according to pitch. Initially pitch was assessed globally and the electrodes placed in approximate pitch order. Then, pitch comparisons were made between adjacent electrodes to ensure that local pitch order was correct. Processor S-Only used 11 electrodes from the surface electrode array in monopolar mode. Processor S+P used the same 11 surface electrode plus the one penetrating electrode, inserted into the processor map in the appropriate pitch location. Processor S-P was a five-channel processor, which used the one penetrating electrode that produced auditory sensations (P16) as a reference electrode paired in a bipolar stimulation mode with five of the 8 penetrating electrodes. Although the other five penetrating electrodes produced nonauditory sensations when they were pulsed stimulated in monopolar mode, they did not produce nonauditory side effects when activated in a bipolar pair with electrode P16. Thus processor S-P was an attempt to localize the current field within the cochlear nucleus. Processor P-Only was a two-channel processor that only utilized two bipolar electrode pairs in the penetrating array.

Speech recognition was assessed on three sets of speech materials: medial consonants (a/C/a), medial vowels (h/V/d), and sentences. At initial stimulation, PABI#1 could not perform at above chance levels on any of these tasks in the sound alone condition, so all processor assessment was done in sound+vision mode.

Figure II-8 presents the results from the four speech processing conditions for each of the three sets of speech materials. Consonant recognition was 37-42% correct with three of the four processors and only 25% correct with

the P-Only processor. Vowel recognition was 54% correct with the S+P and S-Only processors, but only around 40% correct with the S-P and P-Only processors. Sentence recognition was similar for all four processors at 10-16% correct. These scores are all quite low, considering that they include lipreading. It is not unusual for new ABI recipients to demonstrate low performance on these tests at initial stimulation. There was no clear difference between the S+P and S-Only processors, while the P-Only and S-P processors gave poorer performance on at least one speech test. The patient was sent home with four maps and encouraged to switch between them frequently in different listening conditions. The fact that there was no clear difference between processors at initial hookup is not unusual for new ABI recipients. It is common for one processor to eventually emerge as a preferred processor after 3 months experience using processors in various listening conditions. Speech recognition will be remeasured every three months during the first year after initial connection.

Changes in the surgical procedure for future patients

Overall, it was encouraging that one PABI electrode appeared to be in the cochlear nucleus and produced a full range of auditory loudness. It was somewhat disappointing that only one penetrating electrode produced useful auditory percepts, and that the psychophysical characterization of that electrode was similar to the perceptual characteristics of the surface electrodes in the same patient. A review session was held several weeks following the initial stimulation of PABI#1 to review the surgical placement and results. The review was attended by surgeons Derald Brackmann and William Hitselberger, neurosurgery resident Mark Schwartz, Doug McCreery, Audiologist Steve Otto, Bob Shannon, and anatomical consultant Jean Moore. The patient results were reviewed as well as video of the surgery and electrode placement. It was agreed that future PABI surgeries should use a different strategy for targeting the ventral cochlear nucleus and that the insertion tool be modified. The tip of the insertions tool barrel had been angled at 15 degrees to allow the surgeon to achieve the desired placement relative to the tonotopic gradient of the ventral cochlear nucleus. Based on the experience with PABI#,1 it was decided that the angle in the tip was not necessary – the surgeon could achieve the desired insertion angle by elevating the barrel of the insertion tool through the surgical opening. It was also decided to move the slot in the end of the tool barrel that routes the cable from the penetrating array. In PABI#1 the slot was dorsal and the cable from the PABI passed over the ventrolateral edge of the surface array. This may have caused the PABI array to become partly dislodged from the cochlear nucleus. The tool has been modified so that the cable exits from the ventral side of the barrel, and the cable can be routed ventrally over the brainstem, and then recurred and routed through the surgical opening.

Based on a review of the anatomy and the results, we determined that the penetrating array in PABI#1 might have been implanted slightly dorsal and caudal relative to the cochlear nucleus. In PABI#2 the array will be targeted closer to the point of entry of the VIII nerve into the brainstem and closer to the

opening of the lateral recess. In PABI#1 this targeting strategy would have moved the insertion point slightly ventral and rostral from the location at which it was implanted.

At least one additional PABI surgery is anticipated before the end of 2003. The barrel of the PABI insertion tool has been modified as described above and several practice sessions are scheduled to familiarize the neurosurgeon with the new tool design and cable routing procedure.

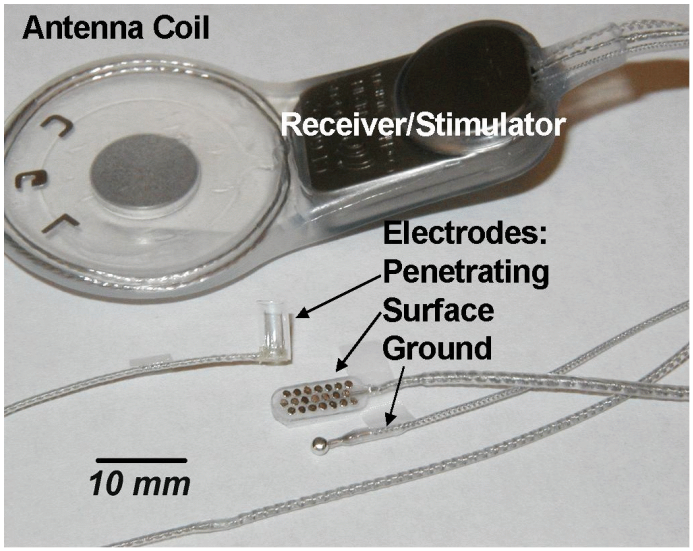

Figure II-1

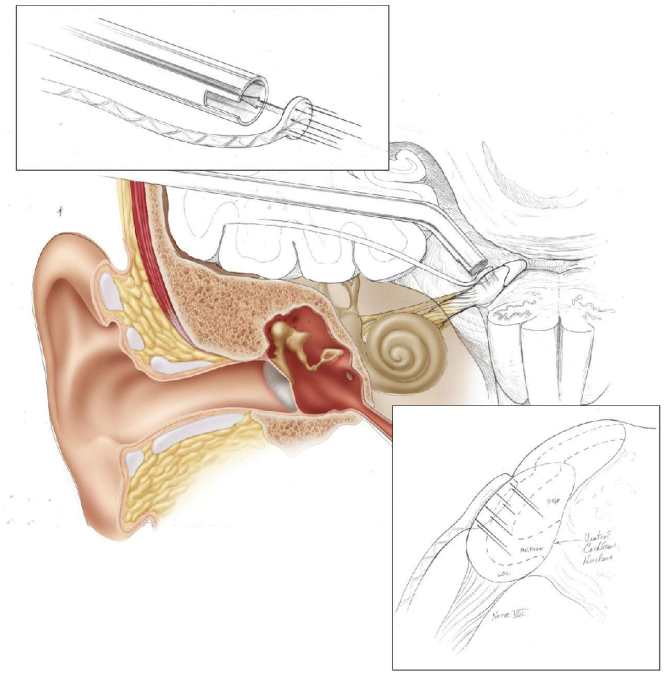

Figure II-2

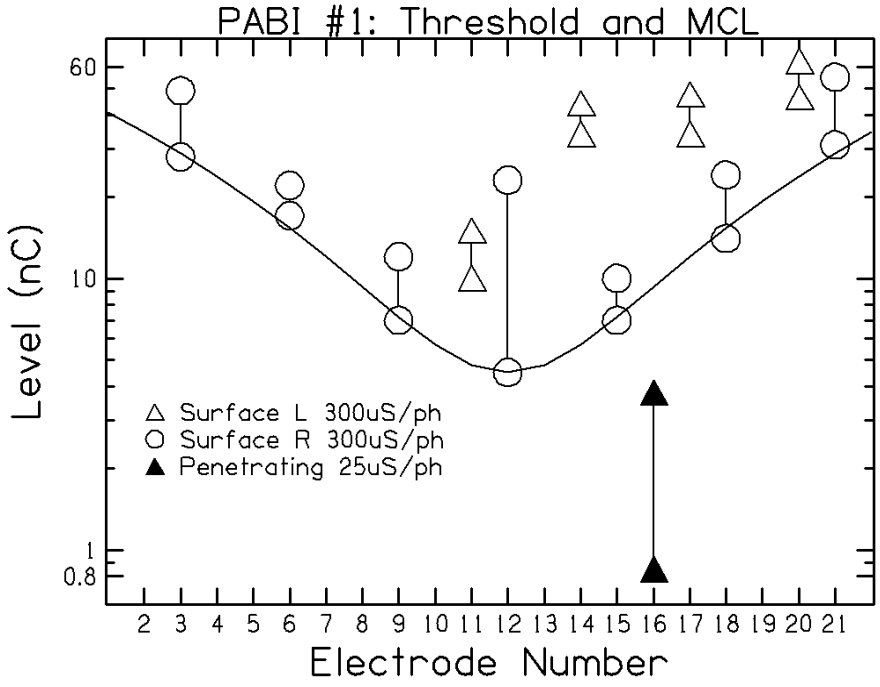

Figure II-3

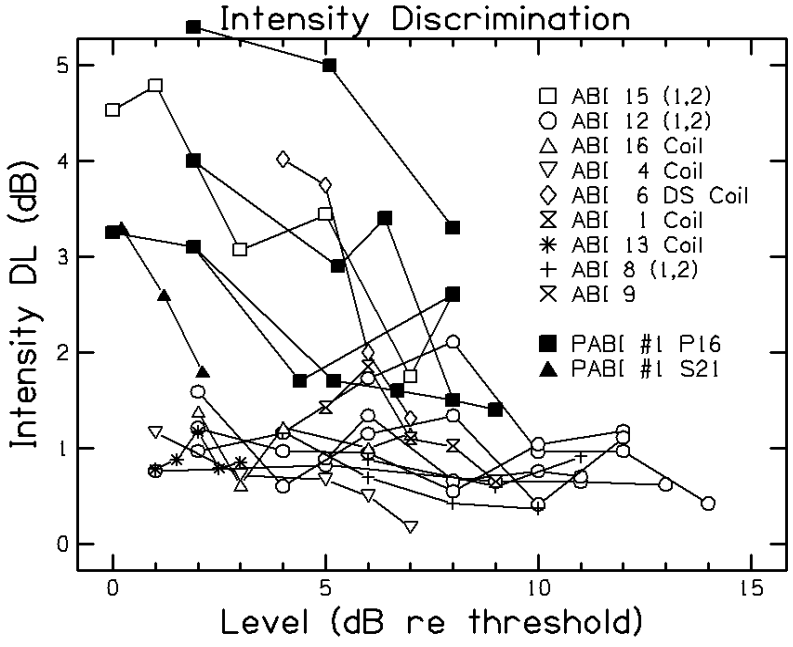

Figure II-4

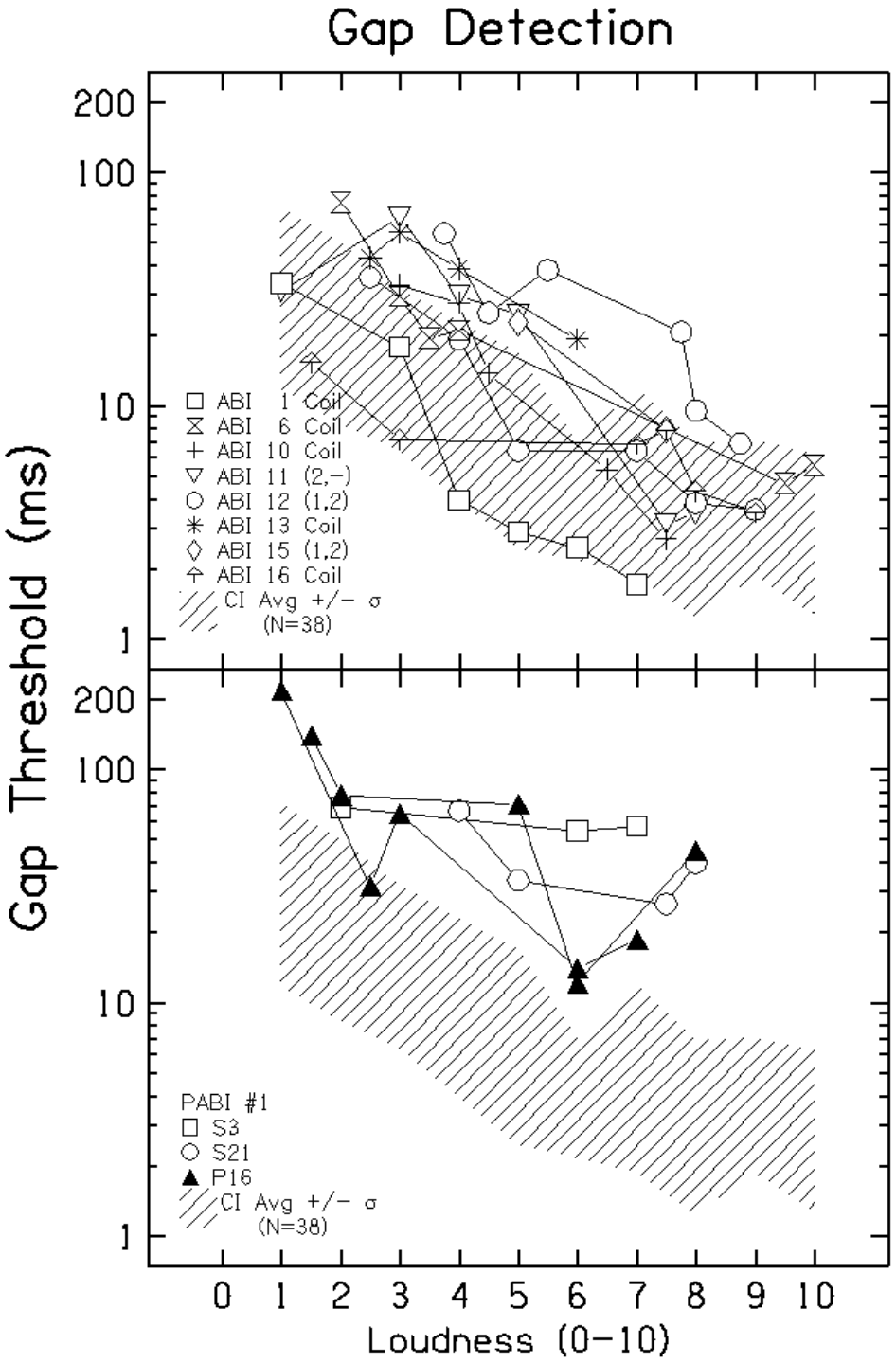
Gap Detection
Gap Threshold (ms)
200
100
10
1
ABI 1 Coil
ABI 6 Coil
ABI 10 Coil
ABI 11 (2,-)
ABI 12 (1,2)
ABI 13 Coil
ABI 15 (1,2)
ABI 16 Coil
CI Avg +/- σ
(N=38)
PABI #1
S3
S21
P16
CI Avg +/- σ
(N=38)
0 1 2 3 4 5 6 7 8 9 10
Loudness (0-10)

Figure II-5

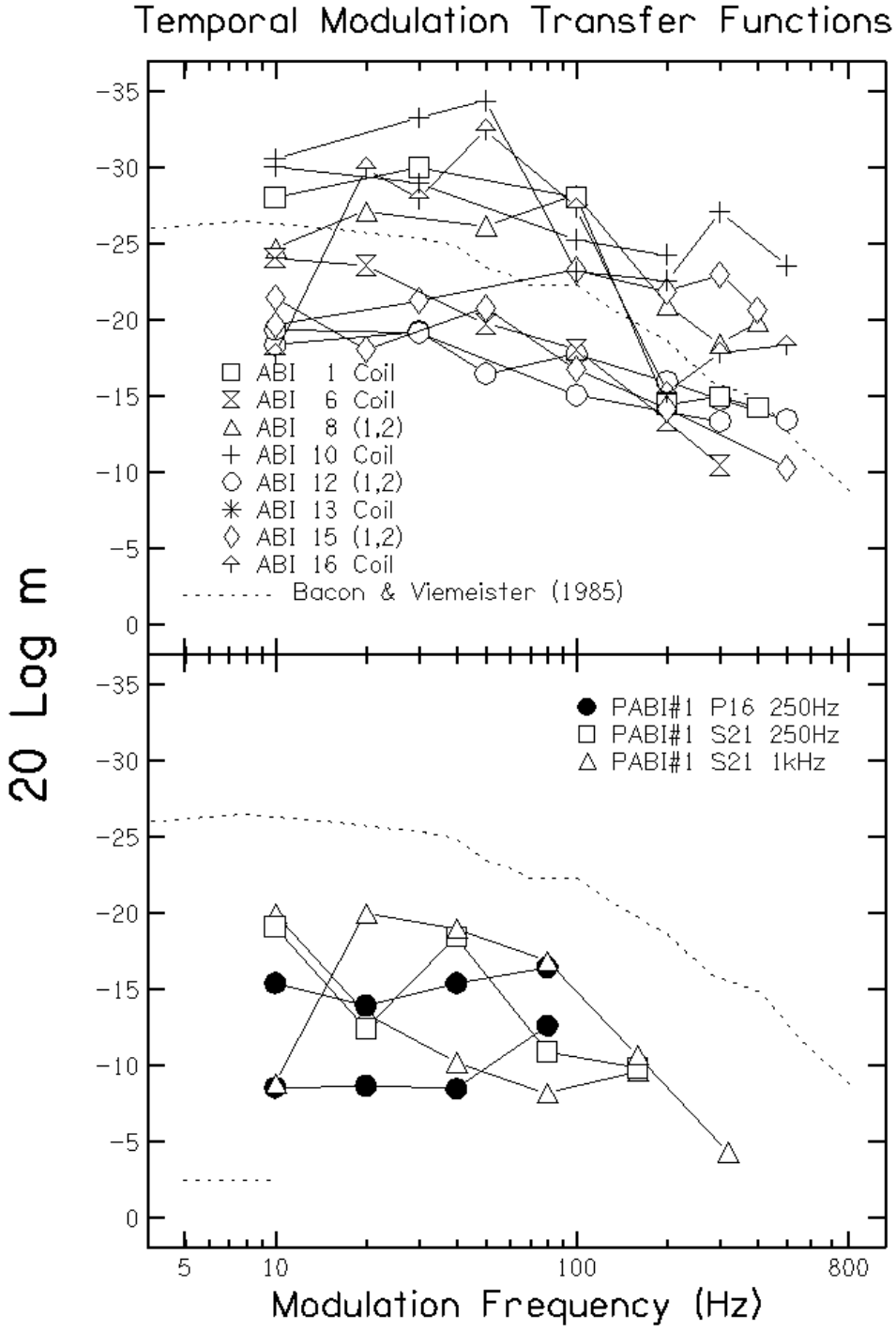
Temporal Modulation Transfer Functions
20 Log m
-35
-30
-25
-20
-15
-10
-5
0
ABI 1 Coil
ABI 6 Coil
ABI 8 (1,2)
ABI 10 Coil
ABI 12 (1,2)
ABI 13 Coil
ABI 15 (1,2)
ABI 16 Coil
Bacon & Viemeister (1985)
PABI#1 P16 250Hz
PABI#1 S21 250Hz
PABI#1 S21 1kHz
5
10
100
800
Modulation Frequency (Hz)

Figure II-6

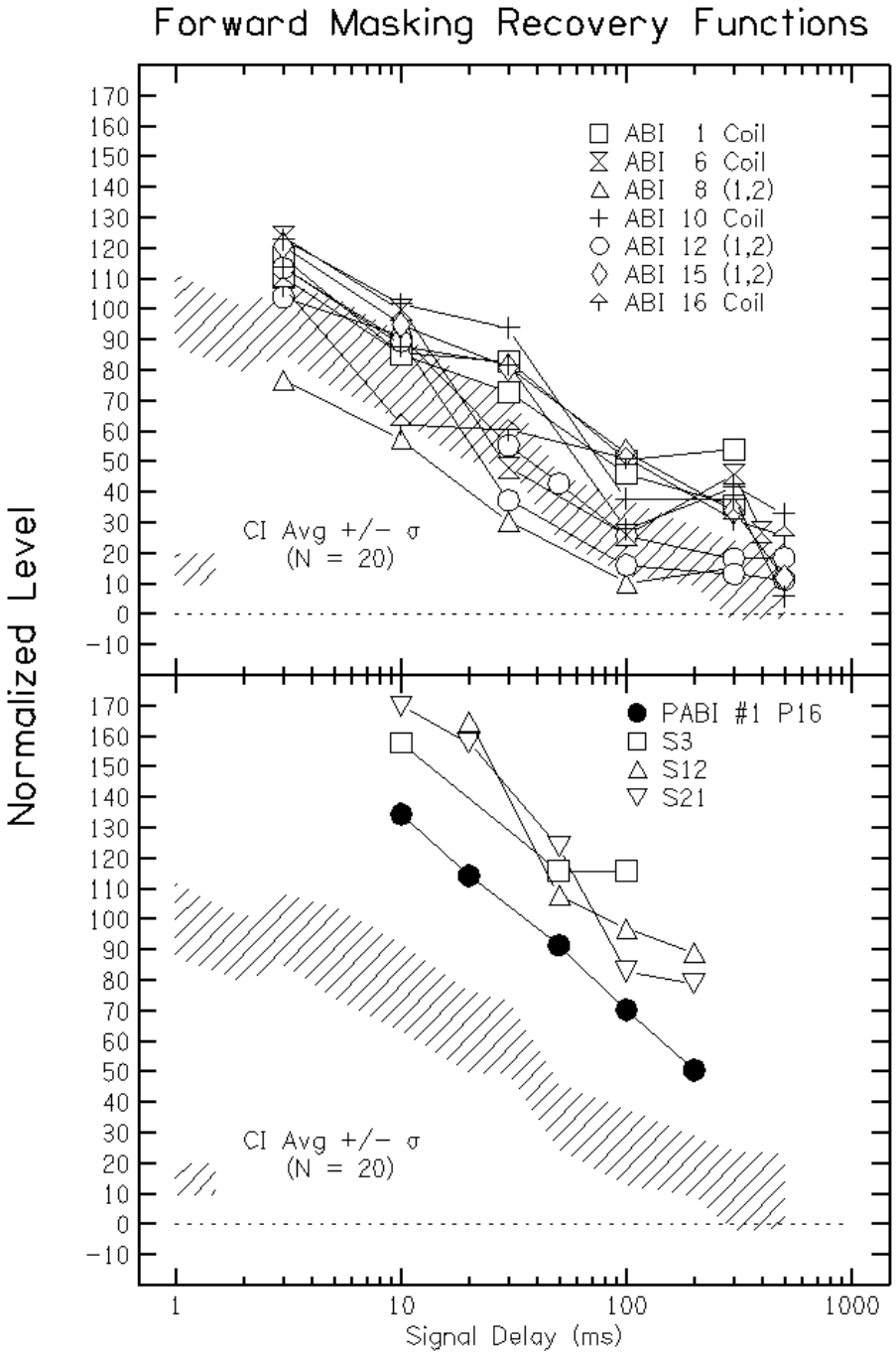
Forward Masking Recovery Functions
Normalized Level
Signal Delay (ms)
ABI 1 Coil
ABI 6 Coil
ABI 8 (1,2)
ABI 10 Coil
ABI 12 (1,2)
ABI 15 (1,2)
ABI 16 Coil
CI Avg +/- σ
(N = 20)
PABI #1 P16
S3
S12
S21
CI Avg +/- σ
(N = 20)

Figure II-7

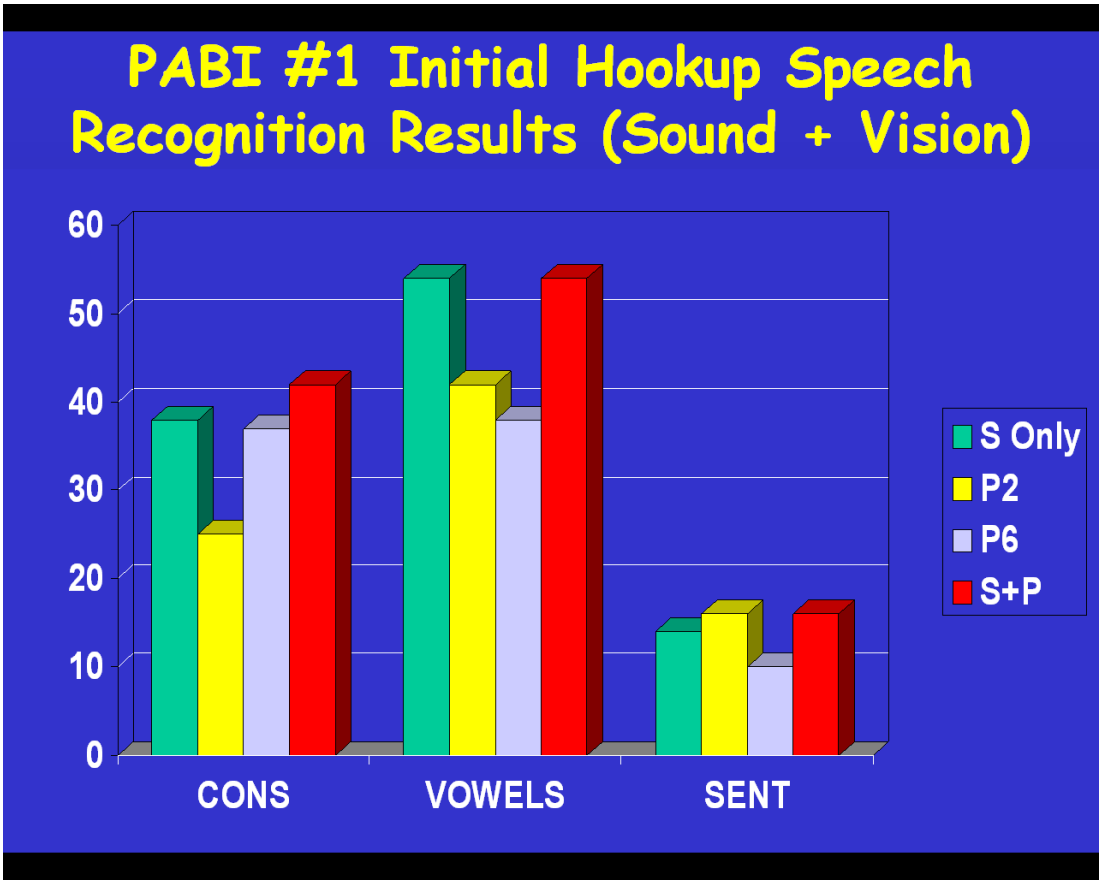
PABI #1 Initial Hookup Speech Recognition Results (Sound + Vision)
60
50
40
30
20
10
0
CONS
VOWELS
SENT
S Only
P2
P6
S+P
Figure II-8

REFERENCES

The artificial voice signal is described in Report P50 of Working Party Q.12/XII, The International Telegraphic and Telephony Consultive Convention (CCITT), Geneva, Switz., (January, 1988)

Bacon, S. P. and N.F. Viemeister. Temporal modulation transfer functions in normal-hearing and hearing-impaired listeners, *Audiology* 24:117-134, 1985.

Brackmann, D.E., W.E. Hitselberger, R.A. Nelson, J.K. Moore, M. Waring, F. Portillo, R.V. Shannon, and F. Telischi. Auditory Brainstem Implant. I: Issues in Surgical Implantation, *Otolaryngology, Head and Neck Surgery* 108:624-634, 1993.

McCreery, D. B., T. G. Yuen, W. F. Agnew, and L. A. Bullara. A characterization of the effects on neuronal excitability due to prolonged microstimulation with chronically implanted microelectrodes. *IEEE Trans Biomed Eng* 44: 931-9, 1997.

McCreery, D. B., T. G. Yuen, and L. A. Bullara. Chronic microstimulation in the feline ventral cochlear nucleus: physiologic and histologic effects. *Hear Res* 149: 223-38, 2000.

McCreery, D. B., W. F. Agnew, and L. A. Bullara. The effects of prolonged intracortical microstimulation on the excitability of pyramidal tract neurons in the cat. *Ann Biomed Eng* 30: 107-19., 2002.

Shannon, R.V. Threshold functions for electrical stimulation of the human cochlear nucleus, *Hearing Res* 40:173-178, 1989.

Shannon, R.V. and S.R. Otto. Psychophysical measures from electrical stimulation of the human cochlear nucleus, *Hearing Res* 47:159-168, 1990.